Structural Durability & Health Monitoring

Tech Science Press

Seismic Reliability Assessment of Inelastic SDOF Systems Subjected to Near-Fault Ground Motions Considering Pulse Occurrence

Jilei Zhou[1,*], Chuansong Sun[1], Xiangjun Dai[1] and Guohai Chen[2]

[1]School of Traffic and Vehicle Engineering, Shandong University of Technology, Zibo, 255049, China
[2]State Key Laboratory of Structural Analysis for Industrial Equipment, Department of Engineering Mechanics, International Research Center for Computational Mechanics, Dalian University of Technology, Dalian, 116023, China
*Corresponding Author: Jilei Zhou. Email: zhjl521@sdut.edu.cn

Abstract: The ground motions in the orientation corresponding to the strongest pulse energy impose more serious demand on structures than that of ordinary ground motions. Moreover, not all near-fault ground motion records present distinct pulses in the velocity time histories. In this paper, the parameterized stochastic model of near-fault ground motion with the strongest energy and pulse occurrence probability is suggested, and the Monte Carlo simulation (MSC) and subset simulation are utilized to calculate the first excursion probability of inelastic single-degree-of-freedom (SDOF) systems subjected to these types of near-fault ground motion models, respectively. Firstly, the influences of variation of stochastic pulse model parameters on structural dynamic reliability with different fundamental periods are explored. It is demonstrated that the variation of pulse period, peak ground velocity and pulse waveform number have significant effects on structural reliability and should not be ignored in reliability analysis. Then, subset simulation is verified to be unbiased and more efficient for computing small reliable probabilities of structures compared to MCS. Finally, the reliable probabilities of the SDOF systems with different fundamental periods subjected to impulsive, non-pulse ground motions and the ground motions with pulse occurrence probability are performed, separately. It is indicated that the ground motion model with the pulse occurrence probability can give a rational estimate on structural reliability. The impulsive and ordinary ground motion models may overestimate and underestimate the reliability of structures with fundamental period much less than the mean pulse period of earthquake ground motions.

Keywords: Near-fault ground motion; strongest pulse energy; pulse occurrence probability; seismic reliability; inelastic SDOF systems

1 Introduction

Intensive researches on engineering characteristics and structural effects of near-fault ground motions arose from the late of last century. Unlike typical far-fault motions, these near-fault ground motions with strong pulses imposed great demands on structures, and have caused severe damage in historic earthquake events [1-4]. Structural damages and collapses motivated earthquake engineers and seismologists to seek for deeper insight into the probabilistic seismic demand and vulnerability of engineering structures under near-fault impulsive ground motions [5-10]. Hereinto, the seismic reliability

or vulnerability assessment of structures under impulsive ground motions is a key procedure. Currently, it is necessary to deal with two major issues for seismic reliability evaluation of civil infrastructures under near-fault strong ground motions. The first is to construct a parametric stochastic model of near-fault ground motion reflecting aleatory uncertainty (record-to-record variability) and epistemic uncertainty (model parameter uncertainty, decision-maker's omissions, or errors), and the other is to suggest an efficient and accurate algorithm for computing the stochastic dynamic responses and seismic reliability of large-scale inelastic structures.

In seismic reliability assessment, many nonlinear response history analyses for every M_w (moment magnitude of earthquake)–R (fault distance) pair in a parameterized stochastic model are needed. Given the fact that time history signals recorded at a specific site constitute a random process which is practically impossible to reproduce, considerable efforts have been taken in recent years on processing actual records so as to become 'representative' of future seismic inputs to the existing or new infrastructures in earthquake-prone regions [11-14]. However, peak parameters (e.g., PGA (peak ground acceleration), PGV (peak ground velocity), etc.) of near-fault pulse-like ground motions present obvious differences in various orientations, which is different from that of ordinary ground motions [5, 15]. The directivity of near-fault ground motion excitation had significant influences on the seismic demands of engineering structures [5, 8, 16]. Unfortunately, the orientation effect of impulsive ground motions has not been considered in the existing stochastic models of near-fault ground motion, which possibly lead to an underestimation of the nonlinear seismic demand on structures [7, 9]. Thus, Yang and Zhou [17] took the orientation of strongest pulses into account and suggested a new stochastic model, which represents the impulsive characteristic of near-fault ground motions, and could generate a number of input samples of impulsive ground motions for the seismic reliability or vulnerability assessments of structures. In addition, the structures located in active tectonic regions will not always be subjected to pulse-like ground motions. Because not each near-source ground-motion record presents a distinct pulse in the velocity time history, it may be argued that near-source records do not always induce non-ordinary seismic demand for structures [18].

Traditional parameterized stochastic models of near-fault ground motion used in seismic reliability assessment do not account for the pulse occurrence probability, and may thus overestimate the seismic reliability of structures at near-fault sites where pulse-like ground motions are expected [7, 9]. Therefore, several researchers proposed pulse probability models at a specific site [18-20], in which the related parameters were fit using lists of pulse-like ground motion records. Iervolino and Cornell [18] compared linear combinations of several predictor variables, and found that source-to-site geometry parameters resulted in the best models for predicting the occurrence probability of a pulse. Shahi and Baker [19] re-fitted these relationships using the new refined list of directivity pulses, which give a better estimate of the probability of observing velocity pulse at a site. In order to correctly assess the seismic reliability of engineering structure at near-fault sites, a probabilistic model of impulsive ground motions considering the occurrence of pulse is developed in this paper, which incorporates the parameterized stochastic model of near-fault ground motions with strongest pulse energy previously established in [17].

Developing appropriate computational methods to estimate seismic reliability or vulnerability of structures and probabilistic seismic hazard has resulted in a variety of associated approaches, such as Monte Carlo simulation method (MCS), the first or second order reliability method (FORM/SORM) [21-24], Latin hypercube sampling (LHS) [25, 26], response surface method [27], etc. Among these approaches, the direct MCS are the widely used one for reliability analysis owing to the ease implementation. However, MCS requires a prohibitively large number of simulations for complicated problems of structural analysis. Thus, it is usually applied for the purpose of a benchmarking in reliability analysis. Furthermore, most of the other approaches are faced with the issues of high nonlinearity of

structures and curse of dimensionality, which limit their scopes of applications. Note that Au and Beck [28, 29] proposed an adaptive stochastic simulation procedure for efficiently computing small failure probabilities of large-scale structure with many random variables, i.e., subset simulation (SS). The SS method expresses failure probability P_f as a product of conditional probabilities that are significantly larger than P_f. These conditional probabilities are estimated by Markov Chain Monte Carlo (MCMC) sampling [30]. Since subset simulation is insensitive to the dimensions of variables and nonlinear degree of limit-state functions, it has been widely applied in the reliability analysis.

This paper aims to present the parameterized stochastic model of near-fault ground motion considering both the strongest pulse energy and pulse occurrence probability, and further evaluate the corresponding seismic reliability of structure. Structural model adopts the inelastic single degree of freedom (SDOF) system that represents a large class of infrastructures such as simple buildings, bridge piers and water towers etc. The inelastic SDOF systems are used only as an example for the application of the proposed methodology, which can be easily extended to reliability estimation of other more complicated structures. Moreover, the influences of impulsive, non-pulse ground motions and the ground motions with pulse occurrence probability on the seismic reliability of SDOF systems are scrutinized.

The rest of this paper is organized as follows. Section 2 gives a brief introduction on the stochastic modeling and synthesis for near-fault impulsive ground motions in the orientation of the strongest pulse. In Section 3, the seismic reliabilities of inelastic SDOF systems with different fundamental periods subjected to near-fault impulsive ground motions are estimated by MCS and SS, and then the influences of variation of stochastic pulse model parameters on structural dynamic reliability are explored. The stochastic ground motion model with pulse occurrence probability is presented in Section 4, and the reliable probabilities of SDOF systems with different fundamental periods respectively subjected to impulsive, ordinary ground motions and the ground motions with pulse occurrence probability are compared in Section 5. Main conclusions are drawn in Section 6. This work provides insightful results regarding the seismic reliability evaluation of structures and reliability-based decision making during the engineering design.

2 Parameterized Stochastic Model for Near-Fault Pulse-Like Ground Motions with the Strongest Pulse Energy

When taking account for the pulse-like or even non-pulse recorded ground motions and their response properties, the orientations of ground motions are important [5]. Shahi [31] proposed an approach to determine the orientation of the strongest pulse extracted from a near-fault ground motion in terms of the wavelet transform.

This approach combines linearly continuous wavelet transform coefficients from two orthogonal components (fault-normal and fault-parallel directions) of a ground motion record to obtain the coefficient for an arbitrary orientation of this ground motion. The wavelet basis function at time t is defined mathematically by

$$\Phi_{s,l}(t) = \frac{1}{\sqrt{s}}\phi\left(\frac{t-l}{s}\right) \tag{1}$$

where $\phi(\cdot)$ and $\Phi_{s,l}(\cdot)$ denote the mother wavelet, the scaled (s) and translated (l) wavelet, respectively, as a function of time (t). The velocity time history in any orientation θ is expressed as

$$V(t,\theta) = V_{FN}(t)\cdot\cos\theta + V_{FP}(t)\cdot\sin\theta \tag{2}$$

in which, $V_{FN}(t)$ and $V_{FP}(t)$ represent velocity time histories in fault-normal and fault-parallel orientations, respectively; $V(t, \theta)$ indicates the velocity time history in an arbitrary orientation away from

$V_{FN}(t)$. The continuous wavelet transform coefficients $c(s, l, \theta)$ [31] for $V(t, \theta)$ at a particular location (l) and scale (s) can be calculated using the following integral

$$\begin{aligned} c(s,l,\theta) &= \frac{1}{\sqrt{s}}\int_{-\infty}^{\infty} V(t,\theta)\phi\left(\frac{t-l}{s}\right)\mathrm{d}t \\ &= \frac{1}{\sqrt{s}}\int_{-\infty}^{\infty} (V_{FN}(t)\cdot\cos\theta + V_{FP}(t)\cdot\sin\theta)\phi\left(\frac{t-l}{s}\right)\mathrm{d}t \\ &= c_1(s,l)\cdot\cos\theta + c_2(s,l)\cdot\sin\theta \\ &= \sqrt{c_1^2(s,l)+c_2^2(s,l)}\cdot\cos(\theta-\beta) \end{aligned} \tag{3}$$

where β means the orientation in which the maximum wavelet coefficient is found, as determined by the following equations

$$c_{\max}(s,l) = \max\left(\sqrt{c_1^2(s,l)+c_2^2(s,l)}\right) \tag{4}$$

$$c_1(s,l) = c_{\max}(s,l)\cdot\cos\beta \quad c_2(s,l) = c_{\max}(s,l)\cdot\sin\beta \tag{5}$$

$$\beta = \tan^{-1}(c_2/c_1) \tag{6}$$

where $c_{\max}(s, l)$ stands for the maximum wavelet coefficient at scale s and location l all over orientations. The corresponding coefficients c_1 and c_2 are achieved according to the row and column location of $c_{\max}(s, l)$, and then the strongest pulse orientation β is determined by Eq. (6). Once the orientation β of the velocity time history with the strongest pulse is known, the resulting velocity time history by a rotation in terms of Eq. (2) is obtained. Note that the maximum wavelet coefficient $c_{\max}(s, l)$ is equal to the energy of the associated wavelet function at scale s and location l. Therefore, the strongest pulse of velocity time history shown in Eq. (2) is also the one with the largest energy which involves *PGV*, pulse period T_p and duration T_d ($T_d = T_p{\cdot}N_c$, and N_c denotes the pulse circle number) of the wavelet function. This type of velocity time history in the orientation of the strongest pulse was used to generate the near-fault impulsive ground motions with the feature of the strongest pulse in our previous paper [17].

For economy of space, we keep the presentation of the method short, as it is described in detail in [17] and references therein. Overall, the model parameters consist of the seismological parameters M_w and R, the additional parameters for the velocity pulse (V_p or PGV, T_p, N_c, the location T_{pk} and phase φ of the pulse) [12, 17]. The velocity time history in the orientation of the strongest pulse contains a high- and low-frequency component. Firstly, a wavelet function [12] is used to fit the low-frequency component to obtain the pulse parameters whose probability distributions can be derived by maximum likelihood method. Then, the statistical power spectral density (PSD) of high-frequency component is fitted by a PSD function to acquire the PSD parameters (i.e., ω_h, ω_g, ξ_g and S_0). Meanwhile, the residual acceleration history of high-frequency component is translated to an envelope function e(t), and the envelope parameters (i.e., τ, α and β) and their corresponding probability distributions can be gained by fitting e(t) and maximum likelihood method respectively. Finally, synthetic ground motions are generated via superposition of a long-period pulse with a stochastic acceleration record generated from a power spectral density function and modulated by an envelope function, whose flowchart as demonstrated in Fig. 1. The Chi-Chi earthquake produced a complete near-fault strong motion dataset available with an average station spacing of 5 km. Thus, this study selects 34 recorded ground motions of the Chi-Chi, Taiwan earthquake (M_w = 7.6) with the closest distance to the fault (R) less than 30 km (except TCU031 with fault distance R = 30.2 km) as the seed impulsive ground motions for statistical parameter analysis. Due to the limited pulse-like recordings with fling-step effect, only the impulsive ground motions with forward directivity effect are considered herein. These velocity time histories of 34 impulsive ground motions and the corresponding fitted pulse parameters are summarized in Tab. 1.

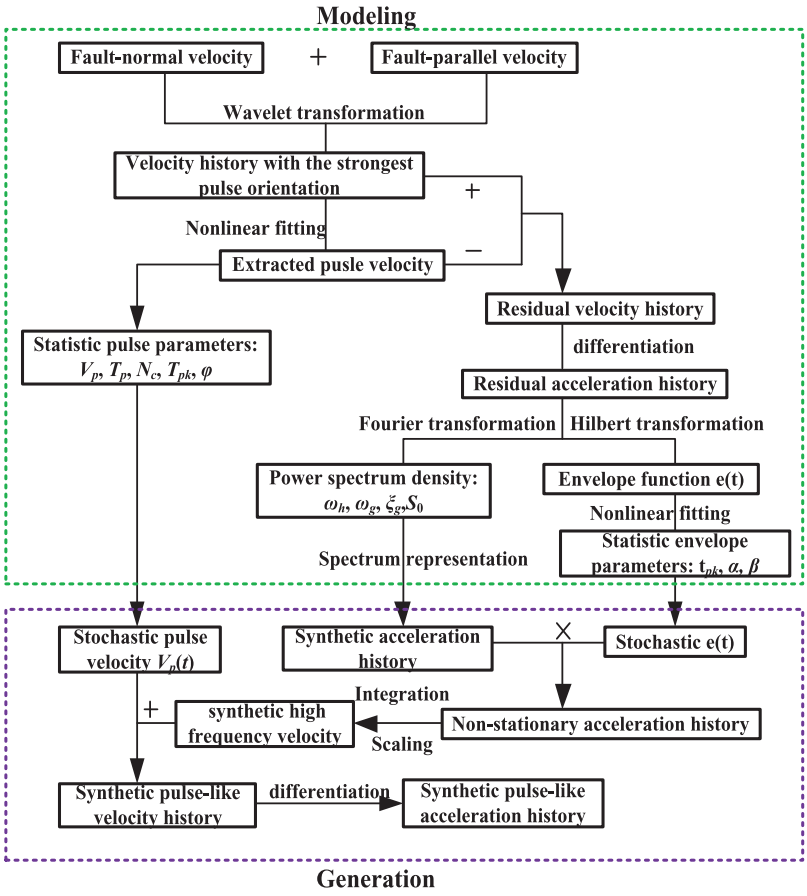

Figure 1: Flowchart for synthesizing acceleration time history of near-fault pulse-like ground motion

A representative sample under the scenario of moment M_w = 7.6 and fault rupture distance R = 5 km is used to generate the synthetic ground motions according to the flowchart in Fig. 1, as shown in Fig. 2. From Fig. 2d, it is indicated that the synthetic velocity time history represents the pulse characteristic of the near-fault ground motions properly, and the corresponding acceleration time history (see Fig. 2e) can be used as the stochastic excitation input for the analysis of structural dynamic reliability in next section.

Table 1: Property parameters of 34 impulsive ground motions and the fitted parameters of velocity pulse model

Ground motion	NGA	R (km)	V_{30} (m/s)	T_p (s)	PGV (cm/s)	V_p (cm/s)	V_{res} (cm/s)	N_c	T_{pk} (s)	φ (rad) (0, 2π)
CHY006	1182	9.8	438	2.36	64.84	57.51	31.88	0.80	17.17	3.20
CHY024	1193	9.6	428	5.25	66.76	45.85	33.60	1.11	17.08	3.76
CHY101	1244	9.9	259	5.19	114.65	83.90	55.43	1.30	20.39	2.20
NSY	1403	13.1	600	7.66	47.42	39.04	25.62	1.45	30.74	1.74
TCU	1462	5.2	473	5.15	47.64	45.65	22.08	0.71	16.31	0.96

(Continued)

Table 1 (continued).

Ground motion	NGA	R (km)	V_{30} (m/s)	T_p (s)	PGV (cm/s)	V_p (cm/s)	V_{res} (cm/s)	N_c	T_{pk} (s)	φ (rad) (0, 2π)
TCU029	1476	28.0	407	4.87	63.69	65.00	31.32	1.18	33.54	2.34
TCU031	1477	30.2	476	5.24	59.89	65.34	25.18	0.96	34.96	2.29
TCU036	1480	19.8	478	4.99	67.90	59.52	28.27	1.39	27.89	0.30
TCU038	1481	25.4	241	6.71	52.18	54.49	31.82	0.82	22.93	4.73
TCU039	1482	19.9	541	7.69	50.53	46.80	29.47	1.84	25.48	3.76
TCU040	1483	22.1	362	6.29	47.80	47.93	16.96	1.14	29.13	3.06
TCU045	1485	26.0	705	8.21	36.27	32.05	36.42	0.86	21.18	1.22
TCU046	1486	16.7	466	7.88	43.02	30.46	19.55	1.12	22.14	5.67
TCU049	1489	3.8	487	9.89	50.81	40.00	27.93	0.86	17.52	2.94
TCU051	1491	7.6	342	8.84	49.32	42.93	31.13	0.66	22.56	2.27
TCU053(1)	1493	6.0	455	6.76	41.74	36.99	40.79	0.99	18.14	4.08
TCU053(2)	1493	6.0	455	8.15	41.74	37.51	39.20	0.98	33.88	6.20
TCU054	1494	5.9	461	8.55	60.47	56.22	38.56	0.56	15.21	3.84
TCU056(1)	1496	10.5	403	5.86	42.05	21.31	35.80	1.63	22.54	2.63
TCU056(2)	1496	10.5	403	7.69	42.05	39.92	27.98	1.18	37.47	3.45
TCU059	1498	17.1	244	7.10	59.53	58.65	44.48	1.02	33.38	4.55
TCU060(1)	1499	9.5	496	6.86	48.58	44.97	45.48	0.83	34.10	5.96
TCU060(2)	1499	9.5	496	7.37	48.58	41.60	48.59	0.98	20.76	2.01
TCU063	1501	9.8	476	5.18	82.50	78.16	39.22	0.89	20.78	0.45
TCU064	1502	16.6	646	7.13	61.20	59.03	25.11	1.87	31.47	2.94
TCU065	1503	0.6	306	4.85	131.05	92.53	86.01	1.55	12.76	2.08
TCU075	1510	0.9	573	5.37	86.51	99.57	29.95	0.61	10.35	4.04
TCU076	1511	2.7	615	4.08	88.67	56.76	38.26	0.69	8.66	2.89
TCU082	1515	5.2	473	7.94	64.91	60.74	35.28	0.61	18.22	3.64
TCU087	1519	7.0	560	9.00	43.78	35.52	21.18	1.12	24.60	1.52
TCU101	1528	2.1	418	8.71	61.19	44.05	32.34	1.23	16.06	0.76
TCU102	1529	1.5	714	8.15	116.06	54.32	72.65	1.15	16.75	0.89
TCU103	1530	6.1	494	7.62	59.72	56.60	35.82	1.00	20.52	1.54
TCU104(1)	1531	12.9	410	6.80	49.75	43.65	49.75	0.81	36.38	5.43
TCU104(2)	1531	12.9	410	6.76	49.75	53.90	39.16	1.03	24.47	0.42
TCU128	1548	13.1	600	7.83	75.59	57.50	27.32	1.34	21.90	5.67
TCU136	1550	8.3	462	8.07	60.93	53.39	31.28	1.07	26.86	3.81
WGK	1595	9.9	259	4.64	76.36	84.24	48.35	1.11	27.03	6.09

Note: (1) and (2) denote the secondary and primary pulses of ground motions.

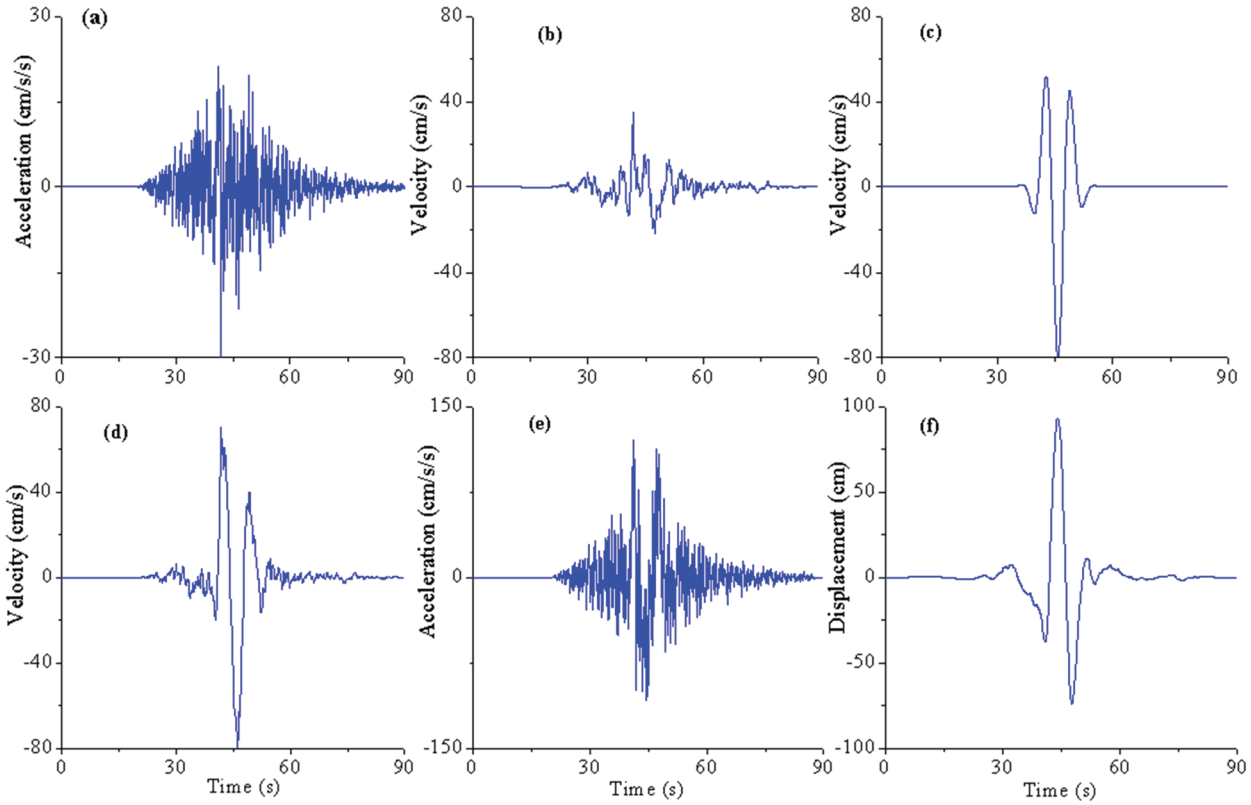

Figure 2: Generation of synthetic ground motions at fault distance R = 5 km (a) stochastic high-frequency acceleration history; (b) normalized velocity history from (a); (c) random velocity pulse; (d) synthetic velocity history through (b) + (c); (e) synthetic acceleration time history; (f) synthetic displacement time history

3 Reliability Assessments of Inelastic SDOF Systems Subjected to Near-Fault Impulsive Ground Motions

Based on the first excursion failure criterion, this section aims at estimating the seismic reliability of inelastic SDOF systems subjected to impulsive ground motions, and how the variability of stochastic pulse parameters affect the seismic reliability of structures with distinct fundamental periods. Generally, reliability analysis requires the calculation of the probabilities that a large number of monotonically increasing limit states are exceeded. Seismic reliability stands for the conditional probability P_r that an earthquake demand parameter (*EDP*) of a structure will not exceed a certain (capacity) threshold, say *edp*, given an intensity level. The seismic intensity can be expressed in terms of magnitude M_w and fault rupture distance R, resulting to a surface $P_r(M_w, R)$ which is defined as

$$P_r(M_w, R) = P(EDP \leq edp | M_w, R) \tag{7}$$

where *EDP* represents the quantities that characterize the system response, for example, the maximum displacement of SDOF system in this paper.

Consider a one-story building, idealized as a cantilever beam system comprising a mass M, a leaf spring of length L, and bending stiffness EI. The system under impulsive ground motion excitation is depicted in Fig. 3. The boundary conditions prevent the rotation of the mass. Then, with the consideration of internal damping coefficient C, the motion equation of SDOF system is expressed as [32]

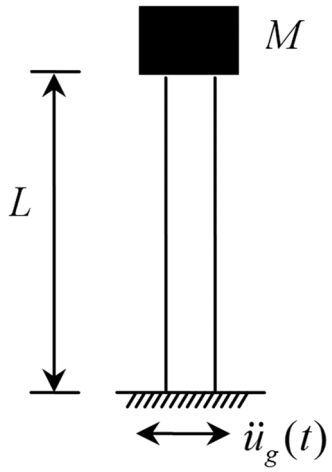

Figure 3: Single degree of freedom shear structure

$$\ddot{X} + 2\zeta\omega_0\dot{X} + \omega_0^2 X + \kappa\omega_0^2 X^3 = -\ddot{u}_g(t) \tag{8}$$

in which the natural frequency for the linear component denotes $\omega_0 = \sqrt{12EI/ML^3}$, the damping ratio is $\zeta = C/(2M\omega_0)$ the coefficient is $\kappa = 36/(35L^2)$, and the excitation $\ddot{u}_g(t)$ is based on the synthetic near-fault ground motions mentioned in Section 2. The reason of using synthetic instead of natural ground motions lies in the limited number of the latter for the range of pairs M_w-R and the need of probabilistic analysis of structures.

3.1 Influence of Variability of Pulse Parameters on Seismic Reliability

For the sake of simplicity, this section just considers impulsive ground motions with various intensities under a specified scenario (M_w, R). Taking the earthquake moment $M_w = 7.6$ and fault rupture distance $R = 5$ km as example, the synthetic pulse-like ground motions with the initial time $t_0 = 0$ s and duration $t_d = 60$ s are generated by using the parameterized stochastic model and procedure in Section 2. The damping ratio is $\zeta = 0.05$, and the fundamental periods of corresponding elastic SDOF system (i.e., the coefficient $\kappa = 0$) are taken as several typical structural periods, such as medium period $T_0 = 1$ s ($\omega_0 = 6.28$ rad/s), medium-long period $T_0 = 3$ s ($\omega_0 = 2.09$ rad/s), long period $T_0 = 6$ s ($\omega_0 = 1.05$ rad/s), respectively.

Hereafter, MCS is performed for a number of nonlinear response history analyses to investigate the effect of the variabilities of impulsive ground motions on the seismic reliability of SDOF structures with different fundamental periods. As a benchmark, the seismic reliability of SDOF system subjected to impulsive ground motions with eight random parameters (5 low-frequency pulse parameters and 3 high-frequency envelope parameters, see Tab. I in [17]) in parameterized stochastic model of near-fault ground motions is calculated. Subsequently, the influence of variability for a single parameter on seismic reliability is separately considered by comparing with the benchmark.

Figure 4a displays the seismic reliability of nonlinear SDOF system with different fundamental periods when the envelope parameters τ, α and β are taken as mean values and stochastic variables respectively, in which the horizontal and vertical axes respectively represent increasing threshold and corresponding seismic reliability or cumulative distribution function (CDF). For every given limit state X, the reliability probability P_r (CDF) of the maximum displacement not exceeding the limit state X can be respectively obtained by MCS, i.e.,

$$P_r = \frac{n(x \le X)}{N} \tag{9}$$

where N is the total number of samples.

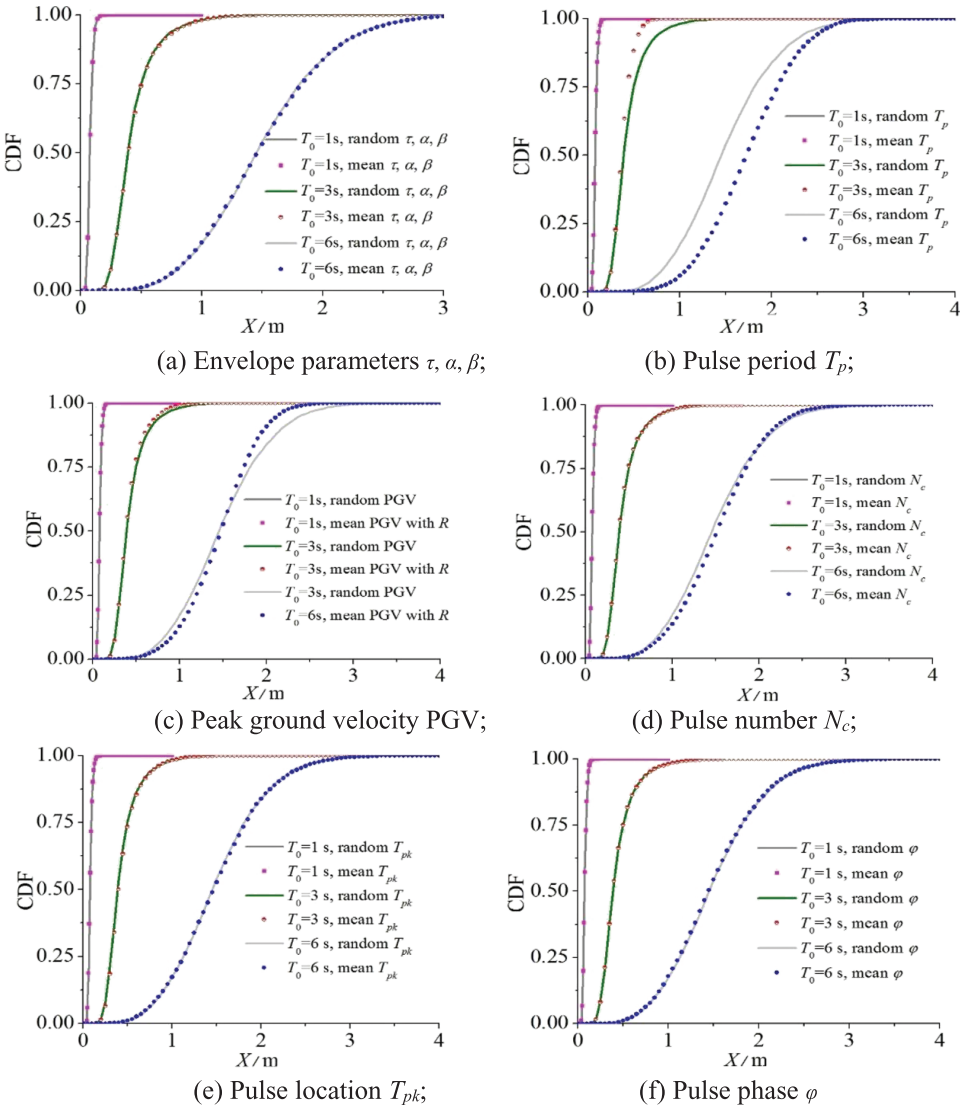

(a) Envelope parameters τ, α, β; (b) Pulse period T_p;

(c) Peak ground velocity PGV; (d) Pulse number N_c;

(e) Pulse location T_{pk}; (f) Pulse phase φ

Figure 4: Influences of model parameters for impulsive ground motion on structural reliability of SDOF systems

It is indicated from Fig. 4a that two types of reliability curves are agreement with each other and the variabilities of envelope parameters have a little effect on structure reliability. In addition, Gavin and Dickinson [33] investigated that high-frequency envelope parameters for impulsive ground motions have little correlation with peak response spectrum, which is in accordance with the results in this paper.

Figures 4b–4f show the impacts of variabilities of low-frequency pulse parameters on seismic reliability of SDOF system with different fundamental periods, which demonstrates that the pulse location T_{pk} and initial phase angle φ are nearly irrelevant to structural reliability, and the period T_p, peak ground velocity PGV and cycle number N_c of pulse are significantly correlated to the reliabilities of long period structures and slightly correlated to that of short period structures ($T_0 < 1$ s). From Fig. 4b, it is noted that the pulse period T_p has a significant influence on the seismic reliability of structures with almost medium-long and long fundamental period. When the pulse period T_p of impulsive ground motions is taken as mean value

Table 2: Random variables for synthetic impulsive ground motions

Parameter type	Parameters	Distribution	Mean	Standard deviation
Pulse parameters	T_p	normal	6.76	1.63
	$\sigma_{\ln PGV}$	normal	0.00	0.26
	N_c	lognormal	0.02	0.29
	T_{pk}	normal	22.04	6.52
	φ	normal	3.04	1.70
Envelope parameters	τ	lognormal	20.67	6.71
	α	lognormal	0.61	0.42
	β	lognormal	−2.53	0.41

Note: The meanings of the parameters in Tab. 2 are respectively pulse period T_p, regression residual $\sigma_{\ln PGV}$ of PGV with rupture distance R, number of circles N_c, pulse location T_{pk}, pulse phase ϕ, and envelope parameters τ, α, β [17]

T_p = 6.76 s [17] (red dotted line) and random variable (green solid line) respectively, there is a remarkable difference between the structural reliabilities under the same limit-state, especially for the structure with the long period T_0 = 6 s. That is because the structure is least susceptible to seismic collapse (i.e., the highest collapse capacities are observed) when the pulse period is approximately equal to the fundamental structure period, such that $T_p/T_0 \approx 1$ [4]. However, for the structure with medium and medium-long fundamental period (T_0 = 3 s for example), the mean value of pulse period for impulsive ground motions is far away from the fundamental period leading increased collapse resistance of structure. Whereas considering the variability of pulse period can make an individual pulse period of synthetic ground motion closed to the fundamental structure period, resulting in decreased collapse resistance of structure.

As shown in Fig. 4c, the impact of PGV variability on seismic reliability of the structure is distinct from that of pulse period. The variability of PGV is slightly correlated to seismic reliability of structure with medium and medium-long fundamental period (T_0 = 1 s and T_0 = 3 s for example) but obviously correlated to that of structure with long fundamental period (T_0 = 6 s). Therefore, considering the PGV variability of impulsive ground motions for a specified scenario (M_w, R) in the seismic design of structure could facilitate to improve the seismic safety of civil infrastructures. On the other hand, the variability of pulse circle number N_c has a similar influence on seismic reliability of SDOF system with that of PGV, as indicated in Fig. 4d.

Furthermore, the seismic reliability of SDOF system subjected to impulsive ground motions with different fault rupture distances is also explored, as depicted in Fig. 5. It is demonstrated from Fig. 5 that the closer to the fault that the building structure is, the easier to be damaged that the structure would be, which is in accordance with field investigation.

Based on these above correlation analyses, herein an impulsive ground-motion model involving a reduced number of random variables is proposed. In order to keep the balance of efficiency and accuracy, the pulse period T_p, peak ground velocity PGV and pulse circle number N_c are taken as random variables, and the other five parameters (envelope parameters T_{pk}, α and β, pulse location T_{pk} and initial phase angle φ) are adopted as mean values for a specified scenario (M_w, R). Therefore, pulse-like ground motions are synthetized through this new type impulsive ground-motion model, which can be regarded as stochastic excitation for structural reliability analysis.

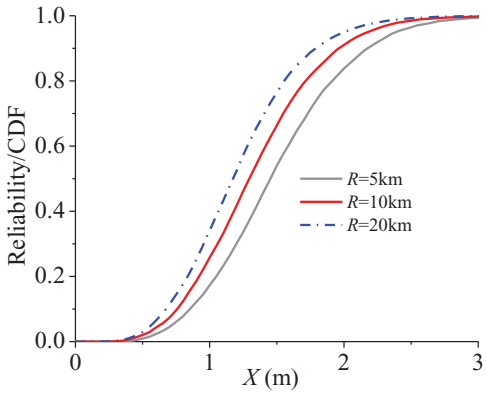

Figure 5: Influence of different fault distance R on structural reliability (T_0 = 6 s)

3.2 Seismic Reliability Assessment of SDOF Systems by Subset Simulation

Checking whether the structure has failed for each sample of ground motion usually requires a run of structure analysis. As is well known, MCS is not computationally efficient for complicated structures, especially for estimating small failure probabilities. In this section, SS is utilized to calculate the seismic reliability of structures instead of MCS. For the convenience of comparison, the SDOF system with long period T_0 = 6 s is chosen as the benchmark model to validate the high efficiency of SS. In the application of SS, the condition failure regions are chosen such that a condition failure probability of p_0 = 0.1 is attained at all simulation level. This is done by choosing an approximate threshold adaptively during the simulation. At each simulation level, N = 500 samples are simulated by the direct MCS. Failure probabilities ranging from 10^{-3} to 1 will be estimated, or in other words, the response level corresponding to failure probabilities as small as 10^{-3} will be estimated.

Figure 6 displays the estimate of failure probability for different limit states obtained by performing SS in a single run. The sample number will adaptively vary with the failure probability and a total of N = 1400 samples, i.e., 1400 runs of dynamic structural analyses, are performed to compute the failure probability. The result computed by direct MCS with 9999 samples (so that the coefficient of variation at a failure probability of 10^{-3} is about 30%) as the exact solution is also shown in Fig. 6 for comparison, which gives an idea of how the results computed by using SS in a single run approximate the 'exact' failure probabilities of MCS. It is demonstrated from Fig. 6 that the failure probability computed by SS agrees well with that by MCS but the sample number of calculations is greatly reduced.

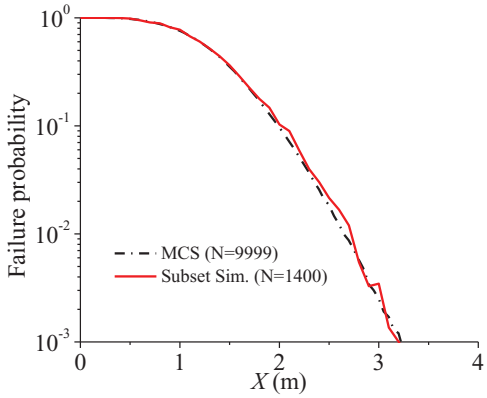

Figure 6: Failure probability estimates computed by SS in a single run

In order to quantitatively assess the statistical property of failure probability estimates produced by SS, 50 independent runs are carried out and the sample mean and sample coefficient of variation of the failure probability estimates are computed, as illustrated in Figs. 7 and 8, respectively. Fig. 7 shows that the sample mean of the failure probability estimates is generally close to the results computed by MCS, except for small failure probabilities near 10^{-3} where the results by MCS are inaccurate due to the number of samples used. It can be concluded from Fig. 7 that the failure probability estimates by SS are practically unbiased. Fig. 8 presents the sample coefficient of variation versus different failure probability levels for the samples of failure probability. Note that the number of samples required by SS at the probability levels $P(F) = 10^{-1}$, 10^{-2}, 10^{-3} are $N = 500$, 950, 1400, respectively. Using $\delta = \sqrt{[1 - P(F)]/P(F)N}$, the coefficient of variation of the Monte Carlo estimator using the same number of samples at probability levels 10^{-1}, 10^{-2}, and 10^{-3} are computed to be 0.13, 0.32, and 0.84, respectively. This figure demonstrates that as the failure probability decreases, the coefficient of variation of the Monte Carlo estimator increases rapidly, while the coefficient of variation of SS increases at a much slower rate. This shows that SS can lead to a substantial improvement in efficiency over MCS when estimating small failure probabilities.

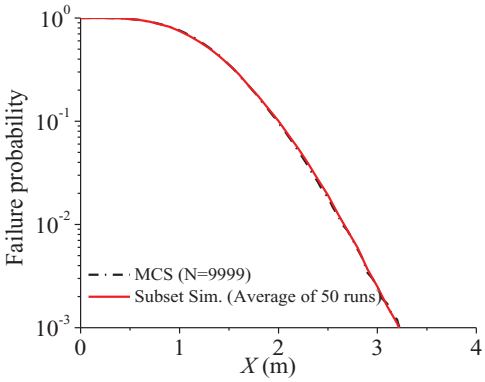

Figure 7: Sample means value of failure probability estimates over 50 runs

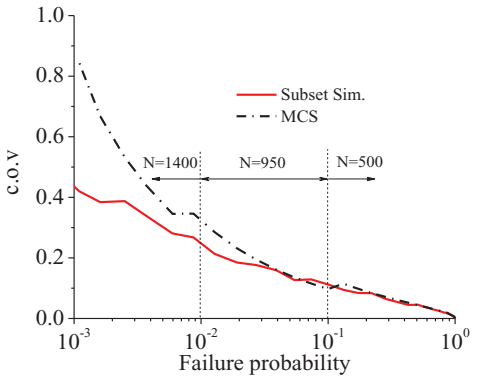

Figure 8: Sample c.o.v of failure probability estimates over 50 runs

4 Parameterized Stochastic Model for Near-Fault Pulse-Like Ground Motions with Pulse Occurrence Probability

Near-fault earthquake ground motions containing large velocity pulses are prone to cause severe demands and collapse on engineering structures and geotechnical systems. Nevertheless, not each near-fault

ground-motion records present an obvious pulse in the velocity time history; it may be argued that near-fault records do not always induce non-ordinary seismic demand for structures. The structures located at near-fault regions may undergo the combined effect of pulse-like and ordinary non-pulse ground motions. Currently, the seismic reliability or collapse fragility analysis of civil structures subjected near-fault ground motions mainly adopts the impulsive ground motions as the seismic inputs, leading to the overestimate of failure probability of structures [7]. Therefore, a model to predict the probability of observing a forward directivity pulse at a near-fault site is necessary.

It has been well established that the forward directivity effect, which tends to produce pulse-like ground motions, is dependent on the source-to-site geometry [1]. However, it is hard to predict the occurrence of pulse-like ground motion at a site because of incomplete information about the source, site and the path of wave propagation that cause this phenomenon. Several researchers have proposed the models for evaluating the probability of pulse at a site [18-20]. These models were fit using lists of pulse-like ground motions, which were used as a surrogate for ground motions with forward directivity pulses. Among these models, the one proposed by Shahi and Baker [19] using the new refined list of directivity pulses is employed in this section, which would give a better estimate of the probability of observing a velocity pulse at a site.

For strike-slip ruptures and non-strike-slip ruptures, the data updated models [19] shown in Eqs. (10) and (11) are respectively adopted in this section to assess the pulse occurrence probability for different source-to-site geometry parameters R, $s(d)$, $\theta(\phi)$ (see Fig. 9)

$$P_r(pulse|R,s,\theta,Strike-slip)=\frac{1}{1+e^{(\alpha_0+\alpha_1 R+\alpha_2\sqrt{s}+\alpha_3\theta)}} \tag{10}$$

and

$$P_r(pulse|R,d,\varphi,non-strike-slip)=\frac{1}{1+e^{\left(\alpha_0+\alpha_1 R+\alpha_2\sqrt{d}+\alpha_3\varphi\right)}} \tag{11}$$

in which parameters α_0, α_1, α_2, α_3 are the fitting relation coefficients which are adjusted to the increased number of near-fault pulse-like records, and taken as $\alpha_0 = 0.457$, $\alpha_1 = 0.126$, $\alpha_2 = -0.244$, $\alpha_3 = 0.013$ for strike-slip ruptures according to the newest dataset in the reference [19].

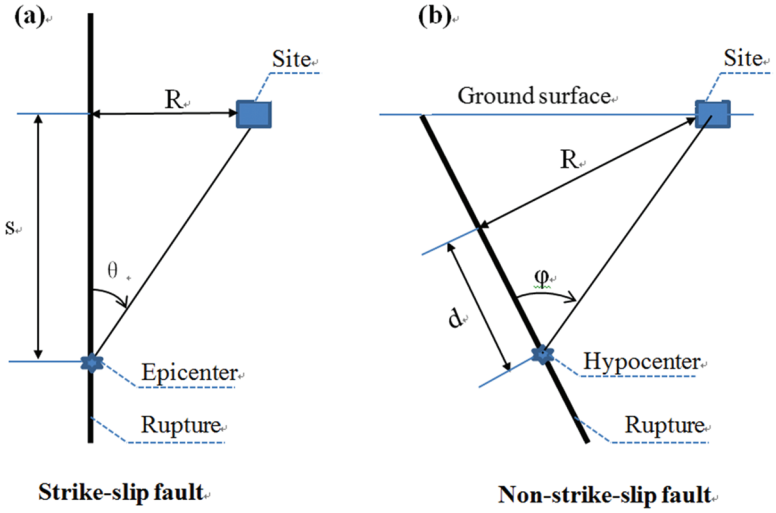

Figure 9: Parameters used to fit the logistic regressions for (a) strike slip and (b) non-strike-slip faults [19]

Thus, the fully probability parameterized stochastic model of near-fault ground motion with the strongest pulse energy and especially considering pulse occurrence probability is completely established. In order to reasonably estimate the seismic reliability of building structures located in active tectonic regions, the combined effect of pulse-like and ordinary non-pulse ground motions should be considered simultaneously. Firstly, the seismic reliabilities of building structures when respectively subjected to pulse-like and ordinary non-pulse ground motions can be obtained according to the impulsive stochastic ground motion model that we proposed in the reference [17] and traditional non-pulse ground motion model [34]. Then, these two cases are combined using the total probability theorem to get the overall probability of seismic reliability. The following section will present the detail process of how to estimate the seismic reliability of building structures located in near-fault regions.

5 Seismic Reliability Assessments of SDOF Systems Under Near-Fault Ground Motions with Pulse Occurrence Probability

According to the statements discussed in Section 4, the seismic reliability of structures located in active tectonic regions are influenced by both impulsive and ordinary no-pulse ground motions and can be expressed as

$$\begin{aligned} P_r(M_w, R, s, \theta) = & P_{pulse}(EDP \le edp|M_w, R) \cdot P_r(pulse|R, s, \theta, Strike{-}slip) + \\ & P_{nopulse}(EDP \le edp|M_w, R) \cdot [1 - P_r(pulse|R, s, \theta, Strike{-}slip)] \end{aligned} \tag{12}$$

The term P_r (M_w, R, s, θ) provides the probability that the EDP of structures located in active tectonic regions not exceeds a value of edp given the source-to-site geometry parameters R, s, θ and occurrence of an earthquake of magnitude M_w. The terms $P_{pulse}(EDP \le edp|M_w, R)$ and $P_{nopulse}(EDP \le edp|M_w, R)$ represent the corresponding reliable probabilities of structures when respectively subjected to impulsive and ordinary non-pulse ground motions under the same source-to-site geometry parameters. The term $P_r(pulse|R, s, \theta, Strike{-}slip)$ represents the probability of the pulse occurrence under the specified source-to-site geometry parameters, which can be obtained from Eq. (10) in Section 4.

In order to obtain the reliable probability of a structure located in active tectonic regions, as displayed in Eq. (12), it is necessary to know the information of source-to-site geometry, the pulse occurrence probability and the seismic input models of near-fault ground motions including impulsive and ordinary ground motions. Suppose that the SDOF systems with the fundamental periods 1 s, 3 s, and 6 s, are located active tectonic zone with the source-to-site geometry parameters R = 5 km, s = 10 km, θ = 27° and subjected to the earthquake of magnitude M_w = 7.6. The other parameters for nonlinear SDOF structure can be seen in Section 3. Firstly, the pulse occurrence probability $P_r(pulse|R, s, \theta, Strike{-}slip)$ at the located site of structure can be acquired by Eq. (10). The pulse-like ground motions are synthesized from the stochastic parametric model of near-fault ground motions in Section 2, and the ordinary non-pulse ground motions are selected according the ground motion prediction equations presented by Boore et al. [34]. Then, the reliable probabilities of inelastic SDOF systems with distinct fundamental periods respectively subjected to impulsive and ordinary ground motions can be obtained according to Eq. (7). Thus, the reliable probability P_r (M_w, R, s, θ) the SDOF systems with different fundamental periods are respectively gained by Eq. (12), as displayed in Figs. 10−12. The horizontal and vertical axes respectively represent the increasing limit-states and the cumulative probabilities of the maximum displacement of SDOF systems not exceeding the limit-state. For the sake of convenient comparison, the reliability terms $P_{pulse}(EDP \ge edp|M_w, R)$ and $P_{nopulse}(EDP \ge edp|M_w, R)$ are also shown in these figures.

Figure 10 demonstrates that the non-pulse ground motions impose the most serious demand on structure with fundamental period far away from the pulse period, leading to the lowest reliability. Nevertheless, the reliability of the structure subjected to impulsive ground motions is the largest. The reliability of the structure

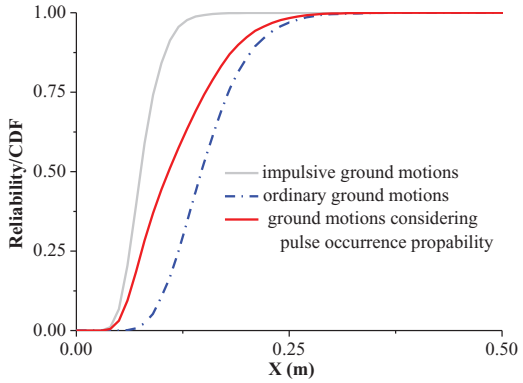

Figure 10: Seismic reliability estimate for SDOF system with fundamental period $T = 1$ s

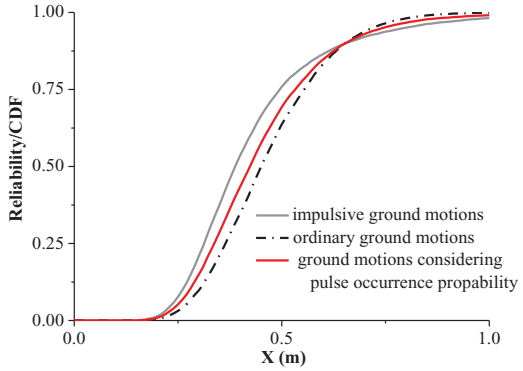

Figure 11: Seismic reliability estimate for SDOF system with fundamental period $T = 3$ s

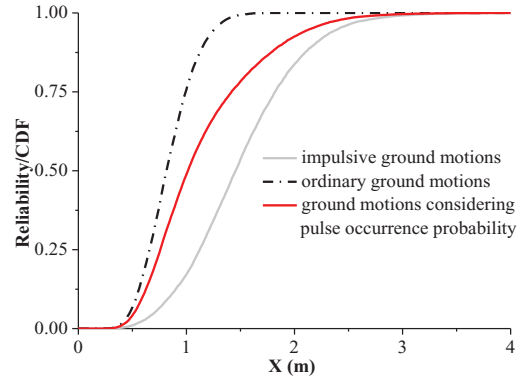

Figure 12: Seismic reliability estimate for SDOF system with fundamental period $T = 6$ s

considering the pulse occurrence probability is between the two others. Because the comprehensive impact of impulse and non-pulse ground motions on the structure is considered, the ground motions model with the pulse occurrence probability can give a rational estimate on structural reliability. Therefore, in the near-fault region, the impulsive and ordinary ground motion models may respectively overestimate and underestimate the reliability of structures with fundamental period much less than the mean pulse period of impulsive ground motions in an earthquake event. With the increasing of fundamental period, the impulsive and ordinary

ground motion models both have important impact on the structure, leading to the similar reliabilities for the structure subjected to three types of ground motion models, as illustrated in Fig. 11. When the fundamental period of structure is close to the mean pulse period of an earthquake event (as seen in Fig. 12), the impulse ground motion model will impose extreme demands on structures, resulting in the lowest reliability among these three types of ground motion models. Thus, in the near-fault region, the impulsive and ordinary ground motion models may respectively underestimate and overestimate the reliability of structures.

6 Conclusions

Near-fault ground motions in the orientation corresponding to the strongest pulse energy impose great demand on structures than that of non-pulse ground motions. Further, not all near-fault ground-motion records exhibit the velocity pulses in the time histories; they usually contain some non-pulse ground motions. Hence, the stochastic parametric models of near-fault ground motion with the strongest energy and pulse occurrence probability are suggested separately in this paper, and the MCS and SS are applied to compute the first excursion reliable probability of nonlinear SDOF systems subjected to the corresponding near-fault ground motions. The seismic reliability analysis demonstrated some of the salient features of inelastic SDOF systems under these types of near-fault ground motion excitations, which can be summarized as follows.

1. The influences of parameter variation of parameterized near-fault ground motion model on structural dynamic reliability with different fundamental periods are investigated. It is indicated that the variation of pulse period T_p, peak ground velocity (PGV) and pulse waveform number N_c have a significant effect on the reliability of SDOF systems, and should not be ignored in reliability analysis. The variations of the other pulse parameters (envelope parameters α, β and τ, pulse location T_{pk}, and pulse phase ϕ) have little influence on structural reliability, and their mean values are just considered in reliability analysis. Moreover, it is illustrated that the subset simulation method is unbiased, and more efficient for computing small failure probabilities of structures compared to MCS.
2. The structures located near-fault regions may undergo the combined effect of pulse-like and non-pulse ground motions. The reliable probabilities of inelastic SDOF systems subjected to impulsive, non-pulse ground motions and the ground motions with pulse occurrence probability are performed, separately. It is demonstrated that the structural reliability can be estimated rationally excited by the ground motion model with the pulse occurrence probability. The impulsive and non-pulse ground motion models may respectively overestimate and underestimate the reliability of structures with fundamental period much less than the mean pulse period of ground motions in a specific earthquake event.
3. With the increasing of fundamental period, the stochastic models for pulse-like and non-pulse ground motion both have important impact on the SDOF systems, leading to the similar reliabilities for the structure subjected to three types of ground motions. For the structure with the fundamental period close to the mean pulse period of an earthquake event, the impulsive and non-pulse ground motion models may underestimate and overestimate the reliability of structures, respectively.

Acknowledgement: The supports of the National Natural Science Foundation of China (Grant Nos. 51478086 and 11672167) and Shandong Province Natural Science Foundation of China (Grant No. ZR2015EL048) are much appreciated. Any opinions, findings, and conclusions or recommendations expressed in this paper are those of the authors and do not necessarily reflect the views of the Natural Science Foundation.

References

1. Somerville, P. G., Smith, N. F., Graves, R. W., Abrahamson, N. A. (1997). Modification of empirical strong ground motion attenuation relations to include the amplitude and duration effects of rupture directivity. *Seismological Research Letters, 68(1),* 199–222. DOI 10.1785/gssrl.68.1.199.

2. Mavroeidis, G. P., Dong, G., Papageorgiou, A. S. (2004). Near-fault ground motions, and the response of elastic and inelastic single-degree-of-freedom (SDOF) systems. *Earthquake Engineering and Structural Dynamics, 33(9),* 1023–1049. DOI 10.1002/eqe.391.
3. Yang, D. X., Pan, J. W., Li, G. (2010). Interstory drift ratio of building structures subjected to near-fault ground motions based on generalized drift spectral analysis. *Soil Dynamics and Earthquake Engineering, 30(11),* 1182–1197. DOI 10.1016/j.soildyn.2010.04.026.
4. Champion, C., Liel, A. (2012). The effect of near-fault directivity on building seismic collapse risk. *Earthquake Engineering and Structural Dynamics, 41(10),* 1391–1409. DOI 10.1002/eqe.1188.
5. Zamora, M., Riddell, R. (2011). Elastic and inelastic response spectra considering near-fault effects. *Journal of Earthquake Engineering, 15(5),* 775–808. DOI 10.1080/13632469.2011.555058.
6. Zhang, S., Wang, G. (2013). Effects of near-fault and far-fault ground motions on nonlinear dynamic response and seismic damage of concrete gravity dams. *Soil Dynamics and Earthquake Engineering, 53,* 217–229. DOI 10.1016/j.soildyn.2013.07.014.
7. Psycharis, I. N., Fragiadakis, M., Stefanou, I. (2013). Seismic reliability assessment of classical columns subjected to near-fault ground motions. *Earthquake Engineering and Structural Dynamics, 42(14),* 2061–2079.
8. Skrekas, P., Giaralis, A. (2013). Influence of near-fault effects and of incident angle of earthquake waves on the seismic inelastic demands of a typical Jack-Up platform. *Proceedings of the 14th International Conference on the Jack-Up Platform Design, Construction and Operation,* London.
9. Dimitrakopoulos, E. G., Paraskeva, T. S. (2015). Dimensionless fragility curves for rocking response to near-fault excitations. *Earthquake Engineering and Structural Dynamics, 44(12),* 2015–2033. DOI 10.1002/eqe.2571.
10. Khoshnoudian, F., Ahmadi, E., Kiani, M., Hadikhan, T. M. (2015). Collapse capacity of soil-structure systems under pulse-like earthquakes. *Earthquake Engineering and Structural Dynamics, 44(3),* 481–490. DOI 10.1002/eqe.2501.
11. Halldórsson, B., Mavroeidis, G., Papageorgiou, A. (2010). Near-fault and far-field strong ground-motion simulation for earthquake engineering applications using the specific barrier model. *Journal of Structural Engineering, 137(3),* 433–444.
12. Dickinson, B. W., Gavin, H. P. (2011). Parametric statistical generalization of uniform-hazard earthquake ground motions. *Journal of Structural Engineering, 137(3),* 410–422. DOI 10.1061/(ASCE)ST.1943-541X.0000330.
13. Motazedian, D., Moinfar, A. (2006). Hybrid stochastic finite fault modeling of 2003, M6.5, Bam earthquake (Iran). *Journal of Seismology, 10(1),* 91–103. DOI 10.1007/s10950-005-9003-x.
14. Mavroeidis, G. P., Papageorgiou, A. S. (2003). A mathematical representation of near-fault ground motions. *Bulletin of the Seismological Society of America, 93(3),* 1099–1131. DOI 10.1785/0120020100.
15. Baker, J. W. (2007). Quantitative classification of near-fault ground motions using wavelet analysis. *Bulletin of the Seismological Society of America, 97(5),* 1486–1501. DOI 10.1785/0120060255.
16. Taskari, O., Sextos, A. (2015). Multi-angle, multi-damage fragility curves for seismic assessment of bridges. *Earthquake Engineering and Structural Dynamics, 44(13),* 2281–2301. DOI 10.1002/eqe.2584.
17. Yang, D. X., Zhou, J. L. (2015). A stochastic model and synthesis for near-fault impulsive ground motions. *Earthquake Engineering and Structural Dynamics, 44(2),* 243–264. DOI 10.1002/eqe.2468.
18. Iervolino, I., Cornell, C. A. (2008). Probability of occurrence of velocity pulses in near-source ground motions. *Bulletin of the Seismological Society of America, 98(5),* 2262–2277. DOI 10.1785/0120080033.
19. Shahi, S. K., Baker, J. W. (2014). An efficient algorithm to identify strong-velocity pulses in multicomponent ground motions. *Bulletin of the Seismological Society of America, 104(5),* 2456–2466. DOI 10.1785/0120130191.
20. Shahi, S. K., Baker, J. W. (2011). An empirically calibrated framework for including the effects of near-fault directivity in probabilistic seismic hazard analysis. *Bulletin of the Seismological Society of America, 101(2),* 742–755. DOI 10.1785/0120100090.
21. Ibarra, L., Krawinkler, H. (2011). Variance of collapse capacity of SDOF systems under earthquake excitations. *Earthquake Engineering and Structural Dynamics, 40(12),* 1299–1314. DOI 10.1002/eqe.1089.

22. Kia, M., Banazadeh, M. (2017). Probabilistic seismic hazard analysis using reliability methods. *Scientia Iranica, 24(3),* 933–941. DOI 10.24200/sci.2017.4077.
23. Kia, M., Banazadeh, M., Bayat, M. (2018). Rapid seismic vulnerability assessment by new regression-based demand and collapse models for steel moment frames. *Earthquake Structures, 14(3),* 203–214.
24. Kia, M., Banazadeh, M., Bayat, M. (2019). Rapid seismic loss assessment using new probabilistic demand and consequence models. *Bulletin of Earthquake Engineering, 17(6),* 3545–3572. DOI 10.1007/s10518-019-00600-9.
25. Celarec, D., Dolšek, M. (2013). The impact of modelling uncertainties on the seismic performance assessment of reinforced concrete frame buildings. *Engineering Structures, 52,* 340–354. DOI 10.1016/j.engstruct.2013.02.036.
26. Vamvatsikos, D. (2014). Seismic performance uncertainty estimation via IDA with progressive accelerogram-wise latin hypercube sampling. *Journal of Structural Engineering, 140(8),* A4014015. DOI 10.1061/(ASCE)ST.1943-541X.0001012.
27. Liel, A. B., Haselton, C. B., Haselton, G. G., Baker, J. W. (2009). Incorporating modeling uncertainties in the assessment of seismic collapse risk of buildings. *Structural Safety, 31(2),* 197–211. DOI 10.1016/j.strusafe.2008.06.002.
28. Au, S. K., Ching, J., Beck, J. L. (2007). Application of subset simulation methods to reliability benchmark problems. *Structural Safety, 9(3),* 183–193. DOI 10.1016/j.strusafe.2006.07.008.
29. Au, S. K., Beck, J. L. (2001). Estimation of small failure probabilities in high dimensions by subset simulation. *Probabilistic Engineering Mechanics, 16(4),* 263–277. DOI 10.1016/S0266-8920(01)00019-4.
30. Papaioannou, I., Betz, W., Zwirglmaier, K., Straub, D. (2015). MCMC algorithms for subset simulation. *Probabilistic Engineering Mechanics, 41,* 89–103. DOI 10.1016/j.probengmech.2015.06.006.
31. Shahi, S. K. (2013). *A probabilistic framework to include the effects of near-fault directivity in seismic hazard assessment*. *(Ph.D. Thesis)*. Stanford University, Stanford, CA.
32. Jin, X. L., Huang, Z. L., Leung, A. Y. T. (2012). Nonstationary seismic responses of structure with nonlinear stiffness subject to modulated Kanai-Tajimi excitation. *Earthquake Engineering and Structural Dynamics, 41(2),* 197–210. DOI 10.1002/eqe.1125.
33. Gavin, H. P., Dickinson, B. W. (2010). Generation of uniform-hazard earthquake ground motions. *Journal of Structural Engineering, 137(3),* 423–432. DOI 10.1061/(ASCE)ST.1943-541X.0000331.
34. Boore, D. M., Stewart, J. P., Seyhan, E., Atkinson, G. M. (2014). NGA-west2 equations for predicting PGA, PGV, and 5% damped PSA for shallow crustal earthquakes. *Earthquake Spectra, 30(3),* 1057–1085. DOI 10.1193/070113EQS184M.